Conservation of the Class I β-*Tubulin* Gene in Human Populations and Lack of Mutations in Lung Cancers and Paclitaxel-resistant Ovarian Cancers[1]

Sanja Šale, Raphael Sung, Peidong Shen, Kristine Yu, Yan Wang, George E. Duran, Jong-Hyeok Kim, Tito Fojo, Peter J. Oefner, and Branimir I. Sikic[2]

Stanford University School of Medicine, Stanford, California 94305-5151 [S. S., Y. W., G. E. D., B. I. S.]; Stanford Genome Technology Center, Palo Alto, California 94306 [R. S., P. S., K. Y., P. J. O.]; and Medicine Branch, Division of Clinical Sciences, National Cancer Institute, Bethesda, Maryland 20892 [T. F., J-H. K.]

Abstract

The goal of this study was to determine the prevalence of sequence variants in the class I *β-tubulin* (clone m40) gene and their occurrence in human tumors and cancer cell lines. DNA was isolated from 93 control individuals representing a wide variety of ethnicities, 49 paclitaxel-naive specimens (16 ovarian cancers, 17 non-small cell lung cancers, and 16 ovarian cancer cell lines), and 30 paclitaxel-resistant specimens (9 ovarian cancers, 9 ovarian cancer cell lines, and 12 ovarian cancer xenografts in nude mice). Denaturing high-performance liquid chromatography and direct sequence analysis detected two silent polymorphisms in exon 4, Leu217Leu (CTG/CTA) and Gly400Gly (GGC/GGT), with minor allele frequencies of 17 and 0.5%, respectively. Five nucleotide substitutions and one single-base deletion were detected in introns 1, 2, and 3 and in the 3′ untranslated region. Analysis of 49 paclitaxel-naive and 30 paclitaxel-resistant specimens revealed no additional polymorphisms in the coding region. In addition, no amino acid replacements were found in chimpanzee, gorilla, and orangutan in comparison to human. Our data demonstrate a very high degree of sequence conservation in class I *β-tubulin,* suggesting that all residues are important in tubulin structure and function. Individual variation in response to treatment with paclitaxel is not likely to be caused by genetic variations in the *β-tubulin* drug target. Moreover, acquired mutations in class I *β-tubulin* are unlikely to be a clinically relevant cause of drug resistance.

Received 10/18/01; revised 11/29/01; accepted 12/3/01.
[1] This work was supported by NIH Grants R01 CA 68217 (to B. I. S.) and R01 HG01932 (to P. J. O.), California Cancer Research Program Grant 99-00561V-10091 (to B. I. S.), and the Margaret Fagin and Beatrice Quackenbush Ovarian Cancer Research Funds.
[2] To whom requests for reprints should be addressed, at Stanford University School of Medicine, Oncology Division, 269 Campus Drive, CCSR-1105, Stanford, CA 94305-5151. Phone: (650) 725-6427; Fax: (650) 736-1454; E-mail: brandy@stanford.edu.

Introduction

Since the mid-1990s, paclitaxel in combination with platinum drugs has been accepted as the standard of care for patients with advanced ovarian cancer. This combination of chemotherapy has also shown efficacy in patients with breast and non-small cell lung cancers (1). Paclitaxel is an antimitotic agent that binds to microtubules and inhibits cell replication by disrupting normal mitotic spindle formation (2, 3). Microtubules are cylindrical structures composed of longitudinal fibers of naturally assembled αβ-tubulin heterodimers (4). Paclitaxel binds stoichiometrically to the *β-tubulin* subunit of the αβ-tubulin heterodimer (5). Upon drug binding, a hydrophobic depression in the paclitaxel binding pocket, located in the intermediate region of *β-tubulin* (Fig. 1), transforms into a hydrophilic surface (6, 7). Microtubules containing *β-tubulin* with such conformational change have an increased lateral polymerization rate and become extraordinarily stable (7, 8). Their inability to rapidly switch between growing and shortening state (9) results in mitotic block (10) and eventually leads to cell death (11–15).

The clinical utility of paclitaxel and similar compounds is limited by the development of drug resistance. More than 75% of women with advanced ovarian cancer ultimately relapse from a clinical remission. The mechanisms by which tumor cells acquire resistance to paclitaxel are not yet fully understood. Selection of mammalian cells with paclitaxel *in vitro* has been shown to result in several changes associated with drug-resistant phenotype. They include expression of the multidrug transporter P-glycoprotein (16–18), alterations in the intracellular target-tubulin (19–23), and alterations in factors that regulate apoptosis (24, 25). Little is known about the prevalence of these mechanisms in the clinical setting. Identification of the precise binding site of paclitaxel to *β-tubulin* by means of electron crystallography (6, 7, 26) has increased interest in the role of simple sequence variations in determining the drug response. Giannakakou *et al.* (27) report two resistant human ovarian cancer cell lines after single-step exposure to paclitaxel. Each cell line acquired a unique mutation in the paclitaxel-binding region of the *β-tubulin* gene. Gonzalez-Garay *et al.* (28) report that mutations in paclitaxel-resistant Chinese hamster ovary cell lines cluster at the site that is likely to be involved in lateral or longitudinal interactions during microtubule assembly. Acquired *β-tubulin* mutations in patients with non-small cell lung cancer have also been reported recently to be associated with paclitaxel resistance (29).

We hypothesized that germ-line sequence variations or acquired mutations in the class I *β-tubulin* gene may contribute to variations in both drug sensitivity and toxicity in the patients undergoing therapy with paclitaxel. Our study focused on class I *β-tubulin,* because this isotype is predom-

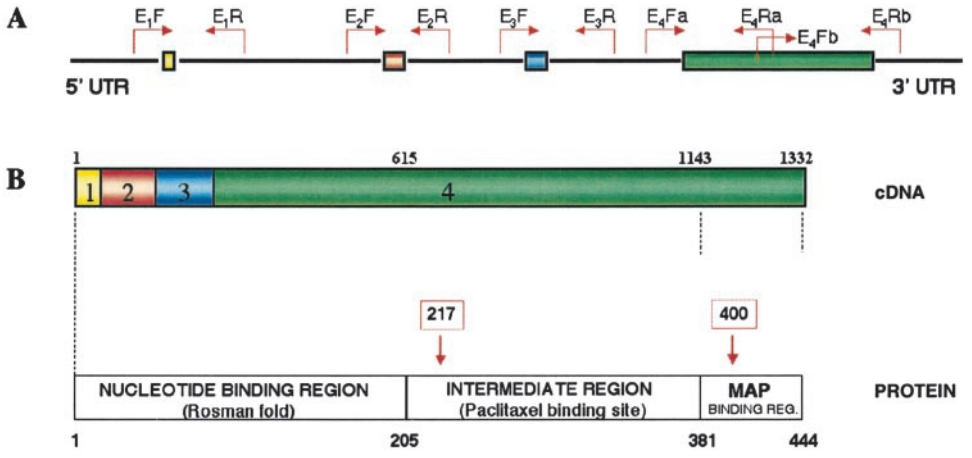

Fig. 1. Schematic representation of the class I *β-tubulin* gene and protein. *A,* genomic DNA exon-intron structure. Location of five pairs of primers specific for the class I *β-tubulin* (m40, class 1) isotype. E_1F, forward primer; E_1R, reverse primer (n = 1–4). Two pairs of primers were used to amplify exon 4. *B,* relationship between cDNA structure and functional domains of the protein. The paclitaxel binding site is situated in the intermediate region and is encoded by exon 4 (615–1143). Two silent SNPs are found at residues 217 and 400. *MAP,* microtubule-associated protein.

inant in ovarian tissue, accounting for 85–99% of total cellular *β-tubulins* (30). To determine the prevalence of SNPs[3] in class I *β-tubulin,* we sequenced genomic DNA isolated from 93 healthy individuals representing a wide variety of ethnicities around the world. In addition, we sequenced DNA isolated from tumor tissue obtained from ovarian and lung cancer patients that have not been exposed previously to paclitaxel. Finally, we analyzed several sets of paclitaxel-resistant human ovarian cancer specimens. These included: (*a*) ovarian tumor tissue obtained from patients who failed paclitaxel therapy; (*b*) paclitaxel-resistant variants selected in ovarian cancer xenografts; and (*c*) ovarian cancer cell lines selected with paclitaxel alone or paclitaxel in combination with the P-glycoprotein inhibitor PSC 833.

Materials and Methods

Human and Ape Variation Panel

Total genomic DNA was extracted through use of a QIAamp DNA Mini kit (Qiagen, Inc., Valencia, CA) from 93 human lymphoblastoid cell lines derived from individuals enrolled according to approved human subject protocols. They represent all continents and a wide variety of ethnicities. The lymphoblastoid lines were obtained by transformation of peripheral blood lymphocytes of these individuals with EBV *in vitro*. Non-human DNA primate samples were derived from fibroblasts and either purchased from Coriell Cell Repositories (Camden, NJ) or obtained from the laboratory of Professor Cavalli-Sforza at the Department of Genetics, Stanford University (Stanford, CA). They included two chimpanzees (*Pan troglodytes*), three lowland gorillas (*Gorilla gorilla*), two orangutans (*Pongo pygmaeus*), and one black-handed spider monkey (*Ateles geoffroyi*).

Human Tumor Specimens, Cell Lines, and Xenografts

The types of human tumor clinical specimens, cell lines, and xenografts used in this study are summarized in Table 1. A detailed description of the origin of these specimens is as follows.

Table 1 Human tumor specimens, cell lines, and xenografts used in this study

Specimen type	Number
No prior paclitaxel exposure (n = 49)	
Ovarian carcinoma clinical specimens	16
Ovarian carcinoma cell lines	16
Lung carcinoma clinical specimens	17
Paclitaxel resistant (n = 30)	
Ovarian carcinoma clinical specimens	9
Ovarian carcinoma lines selected with paclitaxel	6
Ovarian carcinoma lines selected with paclitaxel and PSC 833	3
Ovarian carcinoma xenografts selected with paclitaxel	12

Paclitaxel-naive Samples. Thirteen cryopreserved ovarian carcinoma tumor samples were obtained from an ovarian cancer bank at Stanford. Three ovarian and 17 non-small cell lung cancers were obtained from the Cooperative Human Tissue Network in compliance with institutional guidelines. All of these samples were collected from patients who did not receive paclitaxel treatment and had various stages of disease as well as histological types. Sixteen ovarian carcinoma cell lines (SKOV-3, OVCAR-5, OVCA420, OVCA432, MDAH-2774, SW-626, HEY, OVCAR-8, OVCAR-4, IGROV-1, A2780/1A9, ES-2, MES-OV, OVCA429, OVCA433, and OVCAR-3) were obtained from the American Type Culture Collection repository and other sources.

Paclitaxel-resistant Samples. Nine paclitaxel-resistant ovarian tumor samples were obtained from Rafaella Giavazzi (Instituto Negri, Milan, Italy). Paclitaxel-resistant patients had received one to six cycles of paclitaxel and had progressive disease during paclitaxel therapy or had tumor recurrence within 6 months of the treatment.

In Vitro Paclitaxel Selection

Six ovarian cancer cell lines were chosen for the drug selection studies, based on the following properties: optimal growth characteristics, sensitivity to paclitaxel [measured by

[3] The abbreviations used are: SNP, single nucleotide polymorphism; UTR, untranslated region; DHPLC, denaturing high pressure liquid chromatography; MMR, mismatch repair.

Table 2 Sequences of primers used for amplification and sequencing of class I *β-tubulin* exons in humans and apes

Exon	Species[a]	Primer[b]		Length of sequence (bp)[c]		
		Forward (5′–3′)	Reverse (5′–3′)	Coding	Noncoding	Total
1	H, C, G	TCTCCCTCTCAGAACCTTCCT	GGATAGCGGGTGCAAATG	57	214	271
1	O	TCCAACCTTCCAGCCTGC	GCAAATGCCCCACAACCA	57	142	199
2	H, C, G	GGTTGCAGTGAGCCGAGA	GGAAGGTTTATAGATATACTGGAAAT	109	346	455
2	O	AAAGATGAAATAAAATGGTAGTTGG	CAGCAGGGATCAGAGACTTGTC	109	232	341
3	H, C, G, O	CTTCCCTTCTGCCAGATTTC	GGTATGGAAGATACATGATGTTTC	111	278	389
4A	H, C, G, O	GAAACATCATGTATCTTCCATACC	AGGCATAAAGAAATGGAGACG	506	35	541
4B	H, C, G, O	GTCACCACCTGCCTCCGTT	GGGCACCAGAAAGAAATACAGG	552[d]	190	742[d]
Total	H, C, G			1335	1063	2398
Total	O			1335	877	2212

[a] H, human; C, chimpanzee; G, gorilla; O, orangutan.
[b] Primers were designed using clone m40 sequence (GenBank accession number J00314).
[c] Actual length of sequence varies from clone m40 because differences in sequence between human genomic DNA and clone.
[d] This excludes an overlapping sequence with exon 4a.

the 3-(4,5-dimethylthiazol-2-yl)-2,5-diphenyltetrazolium bromide cytotoxicity assay] and no *MDR1* expression. The parental lines were A2780/1A9, ES-2, MES-OV, OVCA429, OVCA433, and OVCAR-3. Drug selection for each cell line was initiated with the concentration of paclitaxel required to inhibit cell growth by 50% (IC_{50}s), and concentrations were increased with the goal of obtaining cells which were at least 10-fold resistant relative to wild-type cell lines. Three cell lines (A2780/1A9, MES-OV, and OVCAR433) were treated with the P-glycoprotein inhibitor PSC 833 (2 μM) in addition to paclitaxel.

***In Vivo* Paclitaxel Selection.** Tumor specimens obtained via laparotomy or paracentesis from patients with ovarian cancer were established and maintained in nude mice as described by Nicoletti *et al.* (30).

PCR

Primer Design. We designed five pairs of primers specific for class I *β-tubulin* (clone m40) encompassing all exons and adjacent intronic sequences as well as 5′ and 3′ UTRs of the gene (Fig. 1). Primer sequences are shown in Table 2. For primer design and testing of the amplicon specificity, we used the sequence retrievable from GenBank with accession number J00314.

Amplicon Synthesis. Genomic DNA from all samples mentioned above was isolated by standard methods. PCR was carried out in 50-μl reaction volumes containing 50 ng of genomic DNA, 0.2 μM each of forward and reverse primers, 0.1 mM each of the four deoxynucleotide triphosphates, 10 mM Tris (pH 8.3), 50 mM KCl, 2.5 mM $MgCl_2$, 0.1 g/l gelatin, and 1 unit of AmpliTaq Gold Polymerase (PE Biosystems). The touchdown PCR protocol comprised an initial denaturation at 95°C for 10 min to activate AmpliTaq Gold, 14 cycles of denaturing at 94°C for 20 s, primer annealing at 63–56°C with 0.5°C decrements, and extension at 72°C for 1 min, followed by 20 cycles at 94°C for 20 s, 56°C for 1 min, and 72°C for 1 min, and a final 5-min extension at 72°C. Synthesis of appropriately sized PCR reaction products was confirmed by agarose slab gel electrophoresis.

DHPLC Analysis

Detection of simple sequence variation (single-base substitutions, small insertions, or deletions) was performed by means of DHPLC, a highly sensitive and high-throughput technique for mutation screening (31) and direct sequence analysis. The principle behind DHPLC is the differential retention of homo- and heteroduplexes formed during PCR amplification of DNA obtained from a heterozygous individual on a dynamic anion-exchanger under conditions of partial thermal denaturation. To ensure equimolar ratios of homo- and heteroduplex species, unpurified PCR products are subjected to a 3-min 95°C denaturing step, followed by gradual reannealing from 95°C to 65°C over 30 min prior to injection onto an automated HPLC instrument (Transgenomic, San Jose, CA, or Varian Instruments, Walnut Creek, CA). The stationary phase consisted of 2-μm alkylated poly(styrene-divinylbenzene) particles (DNASep; Transgenomic). The mobile phase was 0.1 M triethylammonium acetate buffer, pH 7.0 (Transgenomic), containing 0.1 mM Na4EDTA (Sigma Chemical Co.). Elution of PCR products was accomplished with a linear acetonitrile gradient of 0.5% per min. Heteroduplex mismatches were recognized by the appearance of two or more peaks in the elution profiles under appropriate temperature conditions, which were optimized by computer simulation.[4]

DNA Sequencing

PCR samples were purified with QIAquick spin columns (Qiagen). Both strands were sequenced to determine the location and chemical nature of any polymorphic sites, using the amplimers as sequencing primers and dye-terminator cycle sequencing reagents (Applied Biosystems). Each cycle sequencing reaction contained 3 μl of purified PCR product, 4 μl of dye terminator reaction mix, 0.9 μl of primer (10 μM), and 5.6 μl of H_2O. Cycle sequencing was started at 96°C for 10 min, followed by 30 cycles of 96°C for 10 s, 50°C for 5 s, and 60°C for 4 min. The cycle sequencing reactions were

[4] Available at http://insertion.stanford.edu/melt.html.

purified using Centrifex gel filtration cartridges (Edge Biosystems) and analyzed on an ABI 3700 sequencer.

Inference of Haplotypes from SNPs

Haplotypes were inferred by a maximum-parsimony approach, as described elsewhere (32), for each of the 93 ethnically diverse individuals as well as the 16 ovarian cancer cell lines, 16 human ovarian cancer specimens, and the 17 lung cancer samples, for whom complete genotyping data for all variants had been obtained by direct DNA sequencing. Polymorphic sites from a group of haplotypes or sequences were considered congruent if they could be accommodated by the same phylogenetic typology. In the construction of the tree by maximum parsimony, haplotypes of each individual with multiple polymorphisms were inferred, assuming the smallest number of mutational steps.

Comparison of Nucleotide Diversity among Genes

Mutational analysis of 16 autosomal and 3 Y-chromosome genes was performed in a way similar to that described for class I β-*tubulin,* using gene-specific PCR products spanning the coding and flanking intron sequences for each gene. The human gene names are standard for the online resource LocusLink[5] and their respective Locus IDs are as follows: *ABCB1* (also called *MDR1*), 5243; *AMPD1,* 270; *ATM,* 472; *BRCA1,* 672; *BRCA2,* 675; *CACNA1A,* 773; *COX2* (also called *PTGS2*), 5743; *CSTB,* 1476; *DFFRY* (also called *USP9Y*), 8287; *FBN1,* 2200; *IL4,* 3565; *MMP1,* 4312; *MMP3,* 4314; *MMP12,* 4321; *RB1,* 5925; *SMCY,* 8284; *UTY1,* 7404; *WRN,* 7486; and *XRCC1,* 7515.

Statistical Analysis

Nucleotide diversity was calculated as estimated nucleotide diversity (π, pi), if complete genotypes were available (*AMPD1*, *ATM*, *BRCA1*, *DFFRY*, *MMP1*, *MMP3*, *MMP12*, *SMCY*, class I β-*tubulin,* and *UTY*), or as average heterozygosity (θ, theta), if only heterozygotes were known (*ABCB1*, *BRCA2*, *CACNA1A*, *COX2*, *CSTB*, *FBN1*, *IL4*, *RB1*, *WRN*, and *XRCC1*). The value of theta is very close to that of pi if Hardy-Weinberg equilibrium is satisfied. In a sample of n chromosomes, pi was calculated from the equation:

$$\pi = \sum_{i<j} \mathrm{pi}_{ij}/n_c$$

where pi_{ij} is the number of nucleotide differences between the ith and the jth DNA sequences and $n_c = n(n-1)/2$ (33). Average heterozygosity/site was calculated by dividing the sum of the relative frequencies of heterozygotes per polymorphic site by the total number of bp screened. Tajima's D statistic (34) was calculated by the equation:

$$D = \frac{d}{\sqrt{\check{V}(d)}}$$

where $d = \pi - S/\mathrm{Ms}_{i=1}^{n-1}/I$, S is the number of segregating nucleotides, and $\check{V}(d)$ is an estimator of the variance of d. The value of D is expected to be 0 for selectively neutral variants and infinite sites in a constant population. A greater-than-expected number of rare variants would result in a negative value of D, indicating either purifying selection or population expansion (35). The P for Tajima's D was taken from Fu and Li (36).

Results

Simple Sequence Polymorphisms in Ethnically Diverse Individuals and Apes. Variations in exons 1, 2, 3, and the first half of exon 4, as well as in the flanking noncoding sequences of the human class I β-*tubulin* gene, were analyzed by DHPLC. The second half of exon 4 was screened for mutations by direct sequence analysis only because the 3′UTR region contains a run of Gs that causes slippage and, consequently, formation of heteroduplexes that may affect the ability of DHPLC to detect any additional mutations present. Because direct sequence analysis was used subsequently to determine allelic state at the polymorphic sites, we could confirm the reported high sensitivity of DHPLC because no additional variants were identified in this part of the screening (33).

In the control group of ethnically diverse individuals representing the five continents (Table 3), we found two silent polymorphisms in exon 4, at nucleotide positions 3376 (Leu217Leu; CTG/CTA) and 3925 (Gly400Gly; GGC/GGT), with minor allele frequencies of 17 and 0.5%, respectively. Both variants had occurred in 4-fold degenerate sites that were also part of a CpG or CpNG site. No amino acid replacements were observed in any of the human samples investigated, and the same was true for chimpanzee, gorilla, and orangutan. This also applied to the first 506 bp of exon 4 that could be amplified and sequenced in spider monkey (data not shown). Several additional nucleotide substitutions were detected in introns 1, 2, and 3 as well as in the untranslated regions of humans and apes (Table 4).

Of the nine variant sites found in humans, five (56%) were transitions, two (22%) were transversions, one was a single-base deletion (11%), and one (11%) was an expansion of a run of Gs. Sequence variation occurred in 2 of 1,335 nucleotides (1 in 668) in the coding regions and 7 of 1109 nucleotides (1 of 158) in the noncoding regions. Two variant sites (22%) were observed only once. The frequency of single changes is much lower than that observed in the *ATM*, *BRCA2*, and *CSTB* genes, where they constituted 60% (37), 59% (38), and 67% of all sites, respectively.[6] It is still lower but more similar to that found in the Werner syndrome gene (*WRN*), in which only 33% of the 58 polymorphisms identified in an identical set of individuals were single changes (39). Four (44%) of the DNA variants were observed in Africa, three of which were also detected in other continents. The percentage of variants discovered in Africa is lower than reported previously for *ATM*, *BRCA1*, *CSTB*, and *WRN*, in which 61, 58, 83, and 71% of all polymorphic sites had been detected in Africa. Particularly small is the percentage of

[5] Internet address: http://www.ncbi.nlm.nih.gov/LocusLink/list.cgi.

[6] L. Svensson and P. J. Oefner, unpublished data.

Table 3 Genotype data for seven polymorphic sites in class I *β-tubulin* obtained for 93 representatives from seven continental regions

Continent (no. of individuals)	Ethnicity (no.)	Nucleotide position of polymorphisms[a]							Inferred haplotypes
		2153	2703	2823	3376	3925	4115	4116	
Africa (n = 16)	Pygmy (3)	A	C	C	G	C	G	C	Ht1
	Pygmy (3)	A	C	T	A	C	T	T	Ht6
	Lissongo (2)	W[b]	C	Y[b]	G	C	G	C	Ht1 and Ht4
	Lissongo (2)	A	C	C	G	C	G	C	Ht1
	San (1)	W	C	Y	G	C	G	C	Ht1 and Ht4
	San (2)	A	C	C	G	C	G	C	Ht1
	Ethiopian (2)	A	C	C	G	C	G	C	Ht1
	Sudanese (1)	W	C	Y	G	C	G	C	Ht1 and Ht4
West Asia (n = 9)	Druze (2)	A	C	C	G	C	G	C	Ht1
	Sephardim (2)	A	C	C	G	C	G	C	Ht1
	Bedouin (2)	A	C	C	G	C	G	C	Ht1
	Palestinian (2)	A	C	C	G	C	G	C	Ht1
	Iranian (1)	A	C	C	G	Y	G	C	Ht1 and Ht3
Indian subcontinent (n = 12)	Brushaski (1)	W	C	Y	G	C	G	C	Ht1 and Ht4
	Brushaski (1)	A	C	C	G	C	G	C	Ht1
	Pathan (1)	A	C	C	G	C	G	C	Ht1
	Sindhi (2)	A	C	C	G	C	G	C	Ht1
	Makrani (1)	A	C	C	G	C	G	C	Ht1
	Hazara (1)	W	C	Y	G	C	G	C	Ht1 and Ht4
	Tamil (1)	A	C	C	G	C	G	C	Ht1
	Pakistan (1)	A	C	C	G	C	G	C	Ht1
	Baluchi (1)	W	C	Y	G	C	G	C	Ht1 and Ht4
	Kalash (1)	A	C	Y	R[b]	C	K[b]	Y	Ht1 and Ht6
	Brahui (1)	A	C	C	G	C	G	C	Ht1
East Asia (n = 20)	Cambodian (2)	A	C	C	G	C	G	C	Ht1
	Cambodian	W	C	T	R	C	K	Y	Ht4 and Ht6
	Atayal	A	C	C	G	C	G	C	Ht1
	Ami	A	C	C	G	C	G	C	Ht1
	Japanese (3)	A	C	C	G	C	G	C	Ht1
	Japanese (1)	A	C	Y	R	C	K	Y	Ht1 and Ht6
	Han Chinese (4)	A	C	C	G	C	G	C	Ht1
	Han Chinese (1)	W	C	T	R	C	K	Y	Ht4 and Ht6
	Han Chinese (1)	A	C	Y	R	C	K	Y	Ht1 and Ht6
	Han Chinese (2)	W	C	Y	G	C	G	C	Ht1 and Ht4
	Laotian (1)	A	C	C	G	C	G	C	Ht1
	Korean (1)	A	C	Y	R	C	K	Y	Ht1 and Ht6
	Yakut (1)	A	C	C	G	C	G	C	Ht1
Oceania (n = 8)	New Guinean (1)	W	C	Y	G	C	G	C	Ht1 and Ht4
	New Guinean (1)	A	C	Y	G	C	K	Y	Ht1 and Ht5
	Melanesian (1)	A	C	Y	G	C	K	Y	Ht1 and Ht5
	Melanesian (1)	A	C	C	G	C	G	C	Ht1
	Australian Aborigine (2)	A	C	C	G	C	G	C	Ht1
	Micronesian (1)	A	C	T	R	C	T	T	Ht5 and Ht6
	Samoan (1)	A	C	C	G	C	G	C	Ht1
America (n = 10)	Surui (1)	A	C	C	G	C	G	C	Ht1
	Colombian Indian (2)	A	C	C	G	C	G	C	Ht1
	Mayan (2)	A	C	C	G	C	G	C	Ht1
	Muskogee (1)	A	C	C	G	C	G	C	Ht1
	Navaho (1)	A	C	C	G	C	G	C	Ht1
	Quechua (1)	A	C	C	G	C	G	C	Ht1
	Karitiana (1)	A	C	C	G	C	G	C	Ht1
	Pima (1)	A	C	C	G	C	G	C	Ht1
Europe (n = 18)	German (2)	A	C	C	G	C	G	C	Ht1
	Italian (1)	A	C	Y	R	C	K	Y	Ht1 and Ht6
	Italian (1)	A	C	C	G	C	G	C	Ht1
	Ashkenazi (2)	A	C	C	G	C	G	C	Ht1
	Finn (2)	A	C	C	G	C	G	C	Ht1
	Georgian Republic (1)	A	C	C	G	C	G	C	Ht1
	Georgian Republic (1)	A	Y	C	G	C	G	C	Ht1 and Ht2
	Dane (1)	A	C	C	G	C	G	C	Ht1
	Russian (1)	A	C	C	G	C	G	C	Ht1
	French (2)	A	C	C	G	C	G	C	Ht1
	Utah (2)	A	C	C	G	C	G	C	Ht1
	Amish (1)	A	Y	C	G	C	G	C	Ht1 and Ht2
	Adygei (1)	A	C	C	G	C	G	C	Ht1

[a] Nucleotide positions are given in relation to clone m40 (GenBank accession number J00314).
[b] IUB codes: K, G or T; R, A or G; W, A or T; Y, C or T.

Table 4 Sequence variants found in class I *β-tubulin* in chimpanzee, gorilla, orangutan, and human (including number of heterozygous individuals and geographic location for humans)

Genomic position[a] (location within gene)	Chimpanzee		Gorilla		Orangutan		Human		No. of heterozygotes	Continent[b]
132 (5′UTR)	C	C	T	T	na[c]	na	T	T		
160 (5′UTR)	G	G	C	C	na	na	C	C		
196 (5′UTR)	G	G	G	A	A	A	G	G		
227 (5′UTR)	A	A	G	G	A	A	A	A		
357 (intron 1)	C	C	C	C	G	G	C	C		
387 (intron 1)	A	A	A	A	G	G	A	A		
2128 (intron 1)	G	G	T	T	na	na	G	G		
2138 (intron 1)	A	A	G	G	na	na	G	G		
2153 (intron 1)	A	A	A	A	A	A	A	T	12	Af, As, Oc
2183 (intron 1)	C	C	C	C	T	T	C	C		
2193 (intron 1)	C	C	C	C	G	G	C	C		
2280 (exon 2)	C	C	C	T	C	C	C	C		
2359 (intron 2)	A	A	A	A	C	C	A	A		
2372 (intron 2)	T	T	G	G	T	T	T	T		
2384 (intron 2)	G	G	A	A	G	G	G	G		
2394 (intron 2)	T	T	T	T	C	C	T	delT	1	Af
2395 (intron 2)	C	C	C	C	T	T	C	C		
2404 (intron 2)	T	T	T	T	C	C	T	T		
2406 (intron 2)	A	A	A	A	T	T	A	A		
2429 (intron 2)	T	T	C	C	C	C	C	C		
2430 (intron 2)			insTC	insTC						
2439 (intron 2)	C	C	T	T	C	C	C	C		
2450 (intron 2)	A	A	T	T	A	A	A	A		
2476 (intron 2)	A	A	A	A	A	A	G	G		
2703 (intron 3)	C	C	C	C	C	C	C	T	2	Eu
2723 (intron 3)	T	T	A	A	T	T	T	T		
2754 (intron 3)	A	A	G	G	G	G	G	G		
2805 (intron 3)	A	A	A	A	T	T	A	A		
2823 (intron 3)[d]	T	T	T	T	T	T	T	C	16	Af, As, Oc
2901 (intron 3)	A	A	A	A	G	G	A	A		
2915 (intron 3)	G	G	G	G	A	A	G	G		
2928 (intron 3)	G	G	G	G	C	C	G	G		
2986 (intron 3)	C	C	C	C	T	T	C	C		
3082 (exon 4)	G	G	G	G	C	C	G	G		
3113 (exon 4)	C	C	C	C	T	T	C	C		
3202 (exon 4)	C	C	T	T	C	C	C	C		
3250 (exon 4)	G	G	A	A	G	G	G	G		
3259 (exon 4)	C	C	C	C	C	T	C	C		
3289 (exon 4)	T	T	C	C	C	C	C	C		
3310 (exon 4)	T	T	T	T	C	C	T	T		
3376 (exon 4)[d]	G	G	G	G	G	G	G	A	7	As, Oc
3427 (exon 4)	T	T	T	T	C	C	T	T		
3835 (exon 4)	T	T	C	C	T	T	T	T		
3925 (exon 4)[d]	C	C	C	C	C	C	C	T	1	As
4012 (exon 4)	C	C	C	C	T	T	C	C		
4115 (3′UTR)[d]	G	G	G	G	G	G	G	T	8	As, Oc
4116 (3′UTR)	C	C	C	C	C	C	C	T	8	As, Oc
4130 (3′UTR)	C	C	T	T	C	C	C	C		
4174 (3′UTR)	C	C	C	C	delC	delC	C	C		
4179 (3′UTR)	7G	7G	7G	7G	7G	7G	7–9G	7–9G	47	Global
4184 (3′UTR)	G	G	G	A	G	G	G	G		

[a] Nucleotide positions are given in relation to clone m40 (GenBank accession number J00314).
[b] Af, Africa; As, Asia; Oc, Oceania.
[c] na, not available because orangutan could be amplified only with a different set of primers.
[d] Human DNA variant at CpG or CpNG site.

variant class I *β-tubulin* sites detected exclusively in Africa, 1 of 9 (11%), whereas it was 44, 42, 78, and 24% for *ATM*, *BRCA1*, *CSTB*, and *WRN*, respectively.

Comparison of Class I *β-Tubulin* Orthologues. Table 4 lists the variant sites observed not only in human species but also in the three non-human primate species chimpanzee, lowland gorilla, and orangutan. Although chimpanzee and gorilla could be amplified with the same primers as human, primers for exons 1 and 2 had to be redesigned for orangutan (Table 2), which resulted in a smaller amount of noncoding sequence (877 bp) screened for sequence variation compared to the other three species (1063 bp). As mentioned above, no amino acid replacement sites were detected over 1335 nucleotides of coding sequence, of which 873 were

nondegenerate sites, in the three nonhuman primates. The same was also true for the 506 bp of coding sequence of exon 4 that had been amplified successfully in spider monkey (data not shown). However, there were a total of 11 silent coding sequence differences between human and ape (there were 15 differences between human and spider monkey). Seven of the 11 differences distinguished orangutan from both human as well as chimpanzee and lowland gorilla (Table 4). Two of the seven sites were actually polymorphic in orangutan, with one of the alleles shared by the other species. Three of the 11 differences distinguished gorilla from the other species, whereas only 1 homozygous change was specific for chimpanzee. Eight of the differences were located in the first third of exon 4 between codons 118 and 232, whereas two of the differences were located in the last 20% of exon 4 (codons 369 and 428, respectively), and one in exon 2 (codon 44). Five of the differences had occurred at 4-fold degenerate sites, whereas the other six were associated with 2-fold degenerate sites.

Nucleotide Diversity. Nucleotide diversity was calculated from the number of differences between any two randomly chosen sequences. Given the number of segregating sites, the nucleotide diversity of the coding region of class I *β-tubulin* was very low. For the 1335-bp of coding sequence, the value was $1.13 \pm 2.83 \times 10^{-4}$.

There was a large difference between the nucleotide diversities of class I *β-tubulin* in the coding and flanking noncoding regions. The nucleotide diversity of the latter was $7.08 \pm 7.22 \times 10^{-4}$. Whereas most autosomal and Y-chromosomal genes (14 of 20) in our hands (Fig. 2) have similar nucleotide diversity estimates in the protein coding and noncoding regions, with ratios ranging from 1:2.5 to 1:1, in class I *β-tubulin* the ratio is 1:6.3. Only two genes exhibit a greater ratio, *i.e., RB1* and *ATM*, the ratios of which are 1:44 and 1:7.5, respectively. When total nucleotide diversity, including both coding and noncoding sequences, was calculated for African and non-African populations separately, the latter had 2.3 times less sequence diversity ($3.01 \pm 3.66 \times 10^{-4}$) than did the former population ($6.99 \pm 4.28 \times 10^{-4}$). The respective values of nucleotide diversity for African and non-African populations in *ATM, BRCA2,* and *WRN* were: $3.70 \pm 2.71 \times 10^{-4}$ and $2.55 \pm 2.32 \times 10^{-4}$; $3.54 \pm 4.22 \times 10^{-4}$ and $2.84 \pm 2.73 \times 10^{-4}$; and $7.13 \pm 4.09 \times 10^{-4}$ and $4.82 \pm 3.11 \times 10^{-4}$. The generally greater sequence diversity in the African population is consistent with an African origin of anatomically modern human.

Haplotype Analysis. Haplotypes for each individual were inferred by a maximum-parsimony approach, using the genotyping data of all but two polymorphic sites that had been observed to be heterozygous in the set of ethnically diverse individuals. The two exceptions were the 1-bp deletion in intron 2 observed in a single African individual because it could not be assigned unambiguously and the expansion of Gs observed in the 3′UTR region. The genotypes of each individual for the remaining seven polymorphic sites are listed in Table 3. All sites were in complete linkage disequilibrium over 1964 bp. Six haplotypes, Ht1–Ht6, could be inferred, and their phylogenetic relationship is depicted in Fig. 3. A seventh haplotype, Ht0, was hypothesized to be the ancestral haplotype in the phylogeny, because it was identical to the haplotype of the nonhuman primates.

The dominant haplotype is Ht1. Of 282 chromosomes tested, 248 (88%) were observed to carry this haplotype. Haplotypes 2 and 3 are direct derivatives of Ht1, and they were observed twice and once, respectively, in the Middle East and Europe. Ht4–Ht6 form a distinct cluster of haplotypes that are observed in Africa, the Indian Subcontinent, East Asia, and Oceania, as evident from the color coding in Fig. 3.

Paclitaxel-naive Ovarian Specimens. Analysis of 16 ovarian carcinoma tumor samples and 16 ovarian carcinoma cell lines revealed no mutations in the coding region. One of the cell lines (IGROV1) had a novel single nucleotide substitution, a C to G transversion, 121 bp upstream from the mRNA start site (nucleotide position 146 in relation to GenBank accession number J00314). Its effect, if any, on the level of transcription remains to be elucidated. The same applies to a single-base deletion (delT) that was detected in the ovarian cancer cell line 1A9 20 bp upstream from the mRNA start site, resulting in a reduction of a run of As from seven to six. Other than that, 2 of the ovarian cancer tissue specimens (OV18 and OV270) and 1 of the ovarian cancer cell lines (IGROV1) were heterozygous at nucleotide site 2823, a change identified previously in the set of ethnically diverse individuals. Two of those samples (OV18 and IGROV1) were also heterozygous at nucleotide positions 3376, 4115, and 4116, respectively. In accordance with the haplotype data for the ethnically diverse individuals, Ht1 was the dominant haplotype in the ovarian cancer tissue specimens and cell lines with a relative frequency of 92 and 97%, respectively (Fig. 3). In addition, Ht4 was found in a tissue specimen, whereas Ht6 was observed twice, once each in a tissue specimen and in a cell line.

Paclitaxel-resistant Ovarian Specimens. No SNPs or mutations were found in the coding regions of class I *β-tubulin* among 9 paclitaxel-resistant ovarian tumor samples, 12 human ovarian cancer xenografts, and 9 ovarian cancer cell lines selected with paclitaxel alone or in combination with PSC 833.

Lung Cancer Specimens. A novel noncoding polymorphism, a G to A transition, was observed 96 bp downstream of exon 2 (nucleotide position 2403 in relation to GenBank accession number J00314) in one of the 17 patients examined. Another patient was heterozygous at the four known polymorphic sites 2823, 3376, 4115, and 4116. This was also the only patient to carry a haplotype other than Ht1, *i.e.,* Ht6 (Fig. 3).

Discussion

Recently published cellular models of resistance to paclitaxel were associated with point mutations in *β-tubulin* and suggested that such mutations might be a potential cause of resistance to paclitaxel in the clinical setting (27, 28). The goal of this study was to determine the prevalence of sequence variants in the class I *β-tubulin* gene and their potential role in determining responses of patients with ovarian and lung carcinomas to paclitaxel therapy.

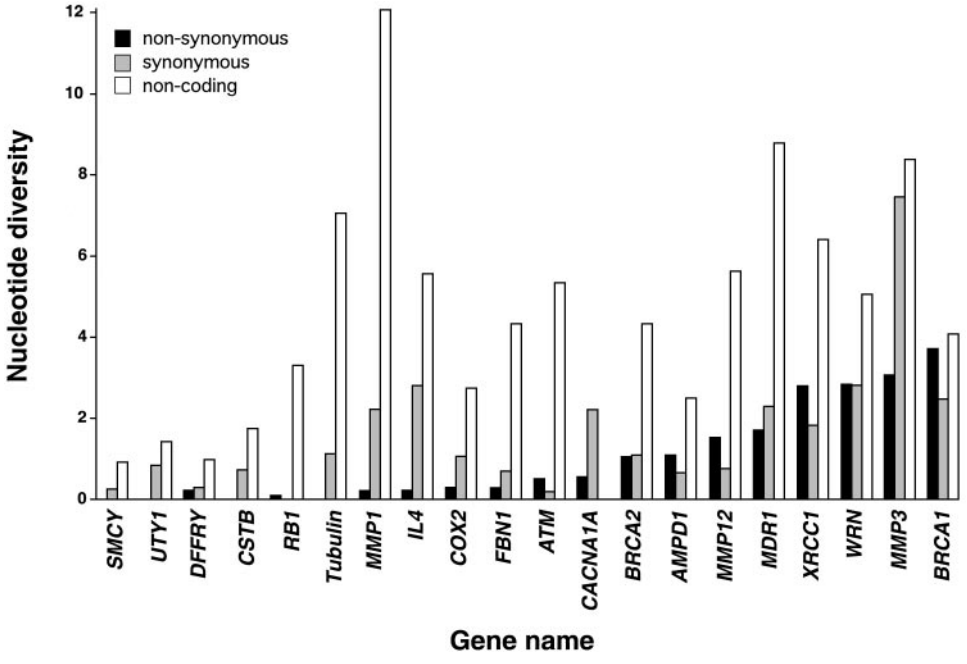

Fig. 2. Nucleotide diversity in the coding and noncoding regions of 17 autosomal and three Y-chromosome genes. Nucleotide diversity, or heterozygosity, was calculated separately for nonsynonymous (■), synonymous (▤), and noncoding sequence variants (□), as described in "Materials and Methods."

Our data show an absence of nonsynonymous SNPs in the entire coding region of class I β-*tubulin* in all 93 normal individuals. Although this finding might seem surprising at first, it is not entirely unexpected. It has been reported previously that there is minimal variation in amino acid sequence of the class I β-*tubulin* isotype among vertebrates (40). Six β-*tubulin* isotypes discovered thus far in vertebrates originate from a common β-*tubulin* ancestor. Divergence of these six isotypes started at the time of the origin of the vertebrates ~450 million years ago. Class III β-*tubulin* diverged from the common ancestor, class II and class IV appeared 330 million years ago, and classes I, V, and VI appeared ~280 million years ago (41). Since then, strong pressure seems to keep certain β-*tubulin* isotypes very conserved. Thus, amino acid sequence variation in one β-*tubulin* isotype between two different vertebrate species is much smaller than the variation between two isotypes in the same organism (40). Our data support this observation. We report 100% identity in class I β-*tubulin* amino acid sequence between humans and nonhuman primates chimpanzee, gorilla, and orangutan. In addition, no amino acid sequence changes were detected in 506 bp of the coding region of class I β-*tubulin* of the spider monkey. Class I β-*tubulin* is the only gene among 20 genes we have studied to date that has shown such a high degree of sequence conservation.

Class I β-*tubulin* has 2.8-fold less sequence diversity than the average in 64,676 coding bp in 15 other autosomal genes (37) and 4.4-fold less than that reported in 135,823 coding bp in 106 human genes (42). Only the *RB1*, *ATM*, *CSTB*, and *FBN1* genes were observed to have lower nucleotide diversity than class I β-*tubulin* in the coding region with values of 0.076×10^{-4}, 0.71×10^{-4}, 0.74×10^{-4}, and 0.98×10^{-4}, respectively (Fig. 2). However, all of the sequence variation in class I β-*tubulin* is limited to two 4-fold degenerate sites. Only one other gene, *CSTB*, is known to have no amino acid replacement sites in the same set of ethnically diverse individuals. However, in contrast to class I β-*tubulin,* nonsynonymous sequence differences have been observed between humans and apes in *CSTB*.[6] Although the Tajima's *D* statistic ($D = -0.78$; $P > 0.05$) fails to support the action of purifying selection on class I β-*tubulin,* the absence of amino acid replacement sites both within human populations as well as between primate species strongly suggests that selection must operate on this gene.

The haplotype analysis presented in Table 2 and Fig. 3 provides evidence for two distinct prehistoric migrations out of Africa. Haplotypes Ht4–Ht6 most likely document the first dispersal of anatomically modern humans along the southern coast of Asia to New Guinea and Australia, where a modern-human burial site dating back ~60,000 years has been found (43). An early dispersal of humans out of Africa is also supported by haplotype data obtained for a chromosome 21 region (32) and the Y-chromosome (44). Most probably, Ht1 left Africa subsequently during the major global expansion of modern humans that occurred ~40,000 years ago (45, 46). Unlike the majority of genes (32, 37, 47, 48), haplotype diversity for class I β-*tubulin* was not observed to be greatest in Africa. Actually, of the six haplotypes, four were observed in Oceania. Three haplotypes each were observed in all other continents, with the exception of the Americas, where haplotype diversity is generally low because of the small number of founders (44, 47, 49). The fairly uniform number of haplotypes observed across all continents is in accordance with selection acting on class I β-*tubulin*, irrespective of geography and environment.

The occurrence of purifying selection is further supported by the global dominance of a single haplotype carried by 88% of all chromosomes analyzed, with a minimum of 69%

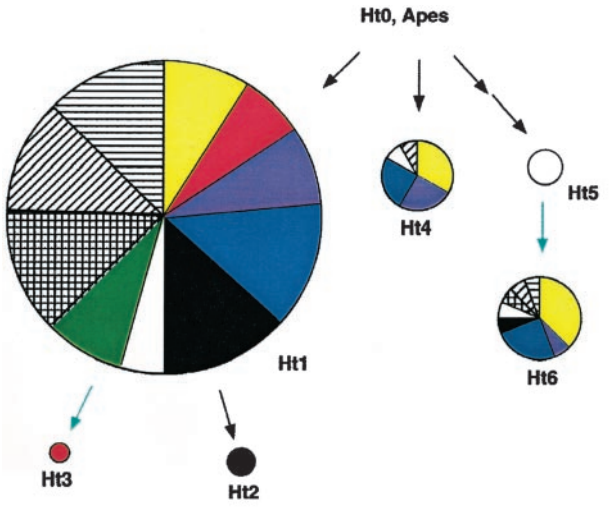

	Ht1	Ht2	Ht3	Ht4	Ht5	Ht6	Total
Africa	22	0	0	4	0	6	32
West Asia	17	0	1	0	0	0	18
India/Pakistan	20	0	0	3	0	1	24
Europe	33	2	0	0	0	1	36
East Asia	33	0	0	3	0	4	40
America	20	0	0	0	0	0	20
Oceania	11	0	0	1	3	1	16
Lung cancer	33	0	0	0	0	1	34
OCCL	31	0	0	0	0	1	32
OCTS	28	0	0	1	0	1	30
Total	248	2	1	12	3	16	282

Fig. 3. Phylogenetic relationships among six class I *β-tubulin* haplotypes. Nonhuman primate sequences were used to determine the root of the phylogeny (*Ht0*). *Arrows,* the number and direction of sequence changes. *Black* and *blue arrows,* noncoding and synonymous polymorphisms, respectively. *Circles* each represent one haplotype. The area of the circle is proportional to the number of chromosomes observed with that haplotype. The *colors* represent seven distinct geographic regions. The ovarian and lung cancer specimens and the ovarian cancer cell lines are included in the haplotype analysis. The haplotype counts are summarized in the table at the *bottom* of the figure. The haplotypes were defined by seven of the nine human variant sites (Table 3), all of which were single-base substitutions. There are 1962 bp between the first and the last polymorphism. Haplotypes are defined as follows (the base change defining a new haplotype is *underlined*): *Ht0,* ACTGCGC; *Ht1,* AC<u>C</u>GCGC; *Ht2,* A<u>T</u>CGCGC; *Ht3,* ACCG<u>T</u>GC; *Ht4,* <u>T</u>CTGCGC; *Ht5,* ACTGC<u>TT</u>; *Ht6,* ACT<u>A</u>CTT.

in Africa and Oceania, and a maximum of 92 and 94% in Europe and West Asia, respectively. Because the sequence diversity in the noncoding regions of class I *β-tubulin* is among the highest of the genes studied (Fig. 2), it is evident that the chromosomal region containing class I *β-tubulin* did not have a generally lower mutation rate. It is more likely that the lower nucleotide diversity in the coding region is a result of selective pressure for maintaining the protein sequence. These data suggest that the prevalent structure of *β-tubulin* is essential for normal cellular function and survival, and that mutations affecting tubulin assembly and/or affinity for tubulin binding proteins are potentially lethal or confer a significant disadvantage.

The lack of nonsynonymous (*i.e.,* amino acid altering) SNPs in the class I *β-tubulin* gene of control individuals indicates that individual variation in response to initial treatment with paclitaxel is not likely to be caused by germ-line variations in this gene. However, genomic instability caused by inactivation or deficiency of human MMR is a hallmark of many cancers and can result in an increased mutation rate (50–52). Defective MMR proteins are present in ~20% of ovarian cancers (53). MMR proteins play a critical role in maintaining the fidelity of the genome by correcting errors in base pairing introduced into the newly synthesized "daughter strand" during DNA replication (54). To determine whether primary tumors have an increased incidence of simple sequence variations in class I *β-tubulin* in comparison with normal tissue, we analyzed 16 ovarian and 17 lung cancer specimens not treated previously with paclitaxel. None of the tumor samples had mutations in the coding region of class I *β-tubulin*. The same was true for 16 nontreated ovarian cancer cell lines. Thus, the absence of mutations in tumor samples prior to therapy argues against a role for preexisting tubulin point mutations as a determinant of the efficacy of taxanes.

It is possible that class I *β-tubulin* mutations might exist in a subclone of cells (<1% of the tumor population) below the limit of detection of our methodology. Those cells would be able to survive during paclitaxel exposure, clonally expand, and become detectable. To test this hypothesis, nine paclitaxel-resistant variants of ovarian cancer cell lines were selected *in vitro* with increasing doses of paclitaxel alone and in combination with the P-glycoprotein inhibitor PSC 833. In addition, 12 ovarian carcinoma xenografts were derived from 3 paclitaxel-naive and 9 paclitaxel-refractory tumors shown previously to have no alterations in the coding regions of class I *β-tubulin*. These xenografts were established in nude mice and selected *in vivo* in the presence of paclitaxel (30). The results from these *in vitro* and *in vivo* selection models show a lack of any mutation in the coding region of class I *β-tubulin*.

Finally, none of the tumors isolated from the paclitaxel-resistant patients exhibited mutations in the coding region of class I *β-tubulin*. Because quantitative reverse transcription-PCR analysis in all paclitaxel-resistant tumor specimens revealed that class I *β-tubulin* constitutes 85–99% of the total cellular *β-tubulin* (30), it is unlikely that potential mutations in other *β-tubulin* isotypes could have had a dominant role in the clinical resistance to paclitaxel.

Two studies have reported mutations in *β-tubulin* after *in vitro* selection with paclitaxel (27, 28). These published examples may be exceptional because of the intrinsic properties of the cell lines used. A2780/1A9 (the only cell line of human origin reported to acquire class I *β-tubulin* mutations upon paclitaxel selection) is a subclone of the ovarian carcinoma cell line A2780. All paclitaxel-selected 1A9 mutants have been reported to have a functionally inactive p53 (55). In a recent study, a novel p53 response element was identified in the promoter region of the *hMSH2* gene of A2780 cells (56). This p53 consensus sequence is unique for the A2780 cell line and is required for *hMSH2* expression (56). Frequent mutations in class I *β-tubulin* in this cell line might therefore result from increased genomic instability caused by inactivation of the MMR system because of the nonfunctional p53. In addition, our data show that 1A9 is the only cell line with a unique single-base deletion (delT) 20 bp upstream

from the class I β-*tubulin* mRNA start site. The functional significance of this deletion is unknown. Moreover, because only the mutant class I β-*tubulin* allele was expressed in both resistant subclones, the wild-type allele had to be silenced (most likely by methylation of the promoter region). Therefore, although point mutations in class I β-*tubulin* can occur, they may require complex additional genetic and epigenetic changes to be functionally relevant.

One of the crucial issues for analyzing sequence variations in any gene that has more than one isotype and/or pseudogene is primer design. Lack of specificity for the class I β-*tubulin* isotype could result in false-positive detection of SNPs or mutations because of COOH-terminal hypervariability among six tubulin isotypes and numerous pseudogenes. For example, primers designed to amplify class I β-*tubulin* may amplify pseudogenes, resulting in a mixture of PCR products with sequence variations that would mimic mutations. This might have been the case in a recent study, where 33% of non-small cell lung cancer samples were reported to have mutations in β-*tubulin* (29). In this study, primers designated TP4 and STP4 have 100% identity not only for class I β-*tubulin* but also for four β-*tubulin* pseudogenes, with the following GenBank accession numbers: V00598, K00841, J00317, and M24191 (29).[7] Similarly, primers with suboptimal homology may amplify sequences other than β-*tubulin*. In the aforementioned study, primer STB4 does not have a 100% match with any gene, including class I β-*tubulin*. The closest match is located on chromosome 16 and is not specific for the whole primer sequence. All but one of the reported mutations were in the COOH-terminal, exon 4 region of the gene, to which these primers were targeted (29). It is likely that these data resulted from the nonspecificity of the PCR primers and do not represent actual β-*tubulin* mutations.

In summary, our data show remarkable conservation of the sequence of the class I β-*tubulin* gene among human individuals, as well as complete conservation of the amino acid sequence of class I β-*tubulin* among several other species of primates. These results suggest that a majority, if not all, amino acids are important for the structure and function of β-*tubulin*. Moreover, mutations in class I β-*tubulin* were not found among 49 ovarian and non-small cell lung carcinoma cases prior to paclitaxel therapy or among 30 ovarian carcinoma cases, cell lines, or xenografts demonstrating resistance to paclitaxel. Alterations in class I β-*tubulin* gene sequence are probably not a significant cause of resistance to taxanes in the clinical setting.

Acknowledgments

We acknowledge the outstanding administrative assistance of Beverly Kennon-Kelley on this project and thank her for her work in the preparation of the manuscript.

References

1. De Vita, V., Hellman, S., and Rosenberg, S. A. Cancer. Principles and Practice of Oncology. Philadelphia, PA: Lippincott, Williams, and Wilkins, 2001.
2. Schiff, P. B., and Horwitz, S. B. Taxol stabilizes microtubules in mouse fibroblast cells. Proc. Natl. Acad. Sci. USA, *77:* 1561–1565, 1980.
3. Jordan, M. A., Wendell, K., Gardiner, S., Derry, W. B., Copp, H., and Wilson, L. Mitotic block induced in HeLa cells by low concentrations of paclitaxel (Taxol) results in abnormal mitotic exit and apoptotic cell death. Cancer Res., *56:* 816–825, 1996.
4. Rao, S., Orr, G. A., Chaudhary, A. G., Kingston, D. G., and Horwitz, S. B. Characterization of the Taxol binding site on the microtubule. 2-(*m*-Azidobenzoyl)Taxol photolabels a peptide (amino acids 217–231) of β-tubulin. J. Biol. Chem., *270:* 20235–20238, 1995.
5. Manfredi, J. J., Parness, J., and Horwitz, S. B. Taxol binds to cellular microtubules. J. Cell. Biol., *94:* 688–696, 1982.
6. Nogales, E., Wolf, S. G., and Downing, K. H. Structure of the αβ-tubulin dimer by electron crystallography. Nature (Lond.), *391:* 199–203, 1998.
7. Snyder, J. P., Nettles, J. H., Cornett, B., Downing, K. H., and Nogales, E. The binding conformation of Taxol in β-tubulin: a model based on electron crystallographic density. Proc. Natl. Acad. Sci. USA, *98:* 5312–5316, 2001.
8. Rowinsky, E. K., and Donehower, R. C. Paclitaxel (Taxol). N. Engl. J. Med., *332:* 1004–1014, 1995.
9. Mitchison, T., and Kirschner, M. Dynamic instability of microtubule growth. Nature (Lond.), *312:* 237–242, 1984.
10. Jordan, M. A., Toso, R. J., Thrower, D., and Wilson, L. Mechanism of mitotic block and inhibition of cell proliferation by Taxol at low concentrations. Proc. Natl. Acad. Sci. USA, *90:* 9552–9556, 1993.
11. Woods, C. M., Zhu, J., McQueney, P. A., Bollag, D., and Lazarides, E. Taxol-induced mitotic block triggers rapid onset of a p53 independent apoptotic pathway. Mol. Med., *1:* 506–526, 1995.
12. Ireland, C. M., and Pittman, S. M. Tubulin alterations in Taxol-induced apoptosis parallel those observed with other drugs. Biochem. Pharmacol., *49:* 1491–1499, 1995.
13. Cheng, L., Zheng, S., Raghunathan, K., Priest, D. G., Willingham, M. C., Norris, J. S., *et al.* Characterizations of paclitaxel-induced apoptosis and altered gene expression in human breast cancer cells. Cell. Pharmacol., *2:* 249–257, 1995.
14. Fan, W. Possible mechanism of paclitaxel-induced apoptosis. Biochem. Pharmacol., *57:* 1215–1221, 1999.
15. Blagosklonny, M. V., and Fojo, T. Molecular effects of paclitaxel: myths and reality. Int. J. Cancer, *83:* 151–156, 1999.
16. Horwitz, S. B., Cohen, D., Rao, S., Ringel, I., Shen, H. J., and Yang, C. P. Taxol: mechanisms of action and resistance. J. Natl. Cancer Inst. Monogr., *15:* 55–61, 1993.
17. Gupta, R. S. Taxol resistant mutants of Chinese hamster ovary cells: genetic, biochemical, and cross-resistance studies. J. Cell. Physiol., *114:* 137–144, 1983.
18. Bhalla, K., Huang, Y., Tang, C., Self, S., Ray, S., Mahoney, M. E., Ponnathpur, V., Tourkina, E., Ibrado, A. M., Bullock, G., *et al.* Characterization of a human myeloid leukemia cell line highly resistant to Taxol. Leukemia (Baltimore), *8:* 465–475, 1994.
19. Cabral, F., Wible, L., Brenner, S., and Brinkley, B. R. Taxol-requiring mutant of Chinese hamster ovary cells with impaired mitotic spindle assembly. J. Cell. Biol., *97:* 30–39, 1983.
20. Schibler, M. J., and Cabral, F. Taxol-dependent mutants of Chinese hamster ovary cells with alterations in α- and β-tubulin. J. Cell. Biol., *102:* 1522–1531, 1986.
21. Kavallaris, M., Kuo, D. Y., Burkhart, C. A., Regl, D. L., Norris, M. D., Haber, M., and Horwitz, S. B. Taxol-resistant epithelial ovarian tumors are associated with altered expression of specific β-tubulin isotypes. J. Clin. Investig., *100:* 1282–1293, 1997.
22. Haber, M., Burkhart, C. A., Regl, D. L., Madafiglio, J., Norris, M. D., and Horwitz, S. B. Altered expression of M β2, the class II β-tubulin isotype, in a murine J774.2 cell line with a high level of Taxol resistance. J. Biol. Chem., *270:* 31269–31275, 1995.
23. Lu, Q., and Luduena, R. F. Removal of βIII isotype enhances Taxol induced microtubule assembly. Cell Struct. Funct., *18:* 173–182, 1993.

[7] Internet address: http: //www.ncbi.nlm.nih.gov/BLAST/.

24. Sumantran, V. N., Ealovega, M. W., Nunez, G., Clarke, M. F., and Wicha, M. S. Overexpression of Bcl-XS sensitizes MCF-7 cells to chemotherapy-induced apoptosis. Cancer Res., *55:* 2507–2510, 1995.
25. Tang, C., Willingham, M. C., Reed, J. C., Miyashita, T., Ray, S., Ponnathpur, V., Huang, Y., Mahoney, M. E., Bullock, G., and Bhalla, K. High levels of p26BCL-2 oncoprotein retard Taxol-induced apoptosis in human pre-B leukemia cells. Leukemia (Baltimore), *8:* 1960–1969, 1994.
26. Nogales, E., Whittaker, M., Milligan, R. A., and Downing K. H. High-resolution model of the microtubule. Cell, *96:* 79–88, 1999.
27. Giannakakou, P., Sackett, D. L., Kang, Y. K., Zhan, Z., Buters, J. T., Fojo, T., and Poruchynsky, M. S. Paclitaxel-resistant human ovarian cancer cells have mutant β-tubulins that exhibit impaired paclitaxel-driven polymerization. J. Biol. Chem., *272:* 17118–17125, 1997.
28. Gonzalez-Garay, M. L., Chang, L., Blade, K., Menick, D. R., and Cabral, F. A β-tubulin leucine cluster involved in microtubule assembly and paclitaxel resistance. J. Biol. Chem., *274:* 23875–23882, 1999.
29. Monzo, M., Rosell, R., Sanchez, J. J., Lee, J. S., O'Brate, A., Gonzalez-Larriba, J. L., Alberola, V., Lorenzo, J. C., Nunez, L., Ro, J. Y., and Martin, C. Paclitaxel resistance in non-small-cell lung cancer associated with *β-tubulin* gene mutations. J. Clin. Oncol., *17:* 1786–1793, 1999.
30. Nicoletti, M. I., Valoti, G., Giannakakou, P., Zhan, Z., Kim, J. H., Lucchini, V., Landoni, F., Mayo, J. G., Giavazzi, R., and Fojo, T. Expression of β-tubulin isotypes in human ovarian carcinoma xenografts and in a sub-panel of human cancer cell lines from the NCI-Anticancer Drug Screen: correlation with sensitivity to microtubule active agents. Clin. Cancer Res., *9:* 2912–2922, 2001.
31. Xiao, W., and Oefner, P. J. Denaturing high-performance liquid chromatography: a review. Hum. Mutat., *17:* 439–474, 2001.
32. Jin, L., Underhill, P. A., Doctor, V., Davis, R. W., Shen, P., Cavalli-Sforza, L. L., and Oefner, P. J. Distribution of haplotypes from a chromosome 21 region distinguishes multiple prehistoric human migrations. Proc. Natl. Acad. Sci. USA, *96:* 3796–3800, 1999.
33. Nei, M. Molecular evolutionary genetics. New York: Columbia University Press, 1987.
34. Tajima, F. Statistical method for testing the neutral mutation hypothesis by DNA polymorphism. Genetics, *123:* 585–595, 1989.
35. Tajima, F. The effect of change in population size on DNA polymorphism. Genetics, *123:* 597–601, 1989.
36. Fu, Y. X., and Li, W. H. Statistical tests of neutrality of mutations. Genetics, *133:* 693–709, 1993.
37. Thorstenson, Y. R., Shen, P., Tusher, V. G., Wayne, T. L., Davis, R. W., Chu, G., and Oefner, P. J. Global analysis of *ATM* polymorphism reveals significant functional constraint. Am. J. Hum. Genet., *69:* 396–412, 2001.
38. Wagner, T. M. U., Hirtenlehner, K. Shen P., Moeslinger, R., Muhr, D., Fleischmann, E., Concin, H., Doeller, W., Haid, A., Lang, A. H., Mayer, P., Petru, E., Ropp, E., Langbauer, G., Kubista, E., Scheiner, O., Underhill, P., Mountain, J., Stierer, M., Zielinski, C., and Oefner, P. Global sequence diversity of *BRCA2*: analysis of 71 breast cancer families and 95 control individuals of world wide populations. Hum. Mol. Genet., *8:* 413–423, 1999.
39. Passarino, G., Shen, P., Van Kirk, J., Lin, A., De Benedictis, G., Cavalli-Sforza, L., Oefner, P., and Underhill, P. The Werner syndrome gene and global sequence variation. Genomics, *71:* 118–122, 2001.
40. Luduena, R. F. Are tubulin isotypes functionally significant? Mol. Biol. Cell, *4:* 445–457, 1993.
41. Colbert, E. H. Evolution of the Vertebrates: A History of the Backboned Animals through Time. New York: John Wiley and Sons, 1980.
42. Cargill, M., Altshuler, D., Ireland, J., Sklar, P., Ardlie, K., Patil, N., Lane, C. R., Lim, E. P., Kalyanaraman, N., Nemesh, J., Ziaugra, L., Friedland, L., Rolfe, A., Warrington, J., Lipshutz, R., Daley, G. Q., and Lander, E. S. Characterization of single-nucleotide polymorphisms in coding regions of human genes. Nat. Genet., *22:* 231–238, 1999.
43. Thorne, A., Grun, R., Mortimer, G., Spooner, N. A., Simpson, J. J., McCulloch, M., Taylor, L., and Curnoe, D. Australia's oldest human remains: age of the Lake Mungo 3 skeleton. Hum. Evol., *36:* 591–612, 1999.
44. Underhill, P. A., Shen, P., Lin, A. A., Jin, L., Passarino, G., Yang, W. H., Kauffman, E., Bonne-Tamir, B., Bertranpetit, J., Francalacci, P., Ibrahim, M., Jenkins, T., Kidd, J. R., Mehdi, S. Q., Seielstad, M. T., Wells, R. S., Piazza, A., Davis, R. W., Feldman, M. W., Cavalli-Sforza, L. L., and Oefner, P. J. Y chromosome sequence variation and the history of human populations. Nat. Genet., *26:* 358–361, 2000.
45. Sherry, S. T., Rogers, A. R., Harpending, H., Soodyall, H., Jenkins, T., and Stoneking, M. Mismatch distributions of mtDNA reveal recent human population expansions. Hum. Biol., *66:* 761–775, 1994.
46. Alonso, S., and Armour, J. A. A highly variable segment of human subterminal 16p reveals a history of population growth for modern humans outside Africa. Proc. Natl. Acad. Sci. USA, *98:* 864–869, 2001.
47. Harding, R. M., Fullerton, S. M., Griffiths, R. C., Bond, J., Cox, M. J., Schneider, J. A., Moulin, D. S., and Clegg, J. B. Archaic African and Asian lineages in the genetic ancestry of modern humans. Am. J. Hum. Genet., *60:* 772–789, 1997.
48. Stephens, J. C., Schneider, J. A., Tanguay, D. A., Choi, J., Acharya, T., Stanley, S. E., Jiang, R., Messer, C. J., Chew, A., Han, J. H., Duan, J., Carr, J. L., Lee, M. S., Koshy, B., Kumar, A. M., Zhang, G., Newell, W. R., Windemuth, A., Xu, C., Kalbfleisch, T. S., Shaner, S. L., Arnold, K., Schulz, V., Drysdale, C. M., Nandabalan, K., Judson, R. S., Ruano, G., and Vovis, G. F. Haplotype variation and linkage disequilibrium in 313 human genes. Science (Wash. DC), *293:* 489–493, 2001.
49. Mesa, N. R., Mondragon, M. C., Soto, I. D., Parra, M. V., Duque, C., Ortiz-Barrientos, D., Garcia, L. F., Velez, I. D., Bravo, M. L., Munera, J. G., Bedoya, G., Bortolini, M. C., and Ruiz-Linares, A. Autosomal, mtDNA, and Y-chromosome diversity in Amerinds: pre- and post-Columbian patterns of gene flow in South America. Am. J. Hum. Genet., *67:* 1277–1286, 2000.
50. Peltomaki, P., Aaltonen, L. A., Sistonen, P., Pylkkanen, L., Mecklin, J. P., Jarvinen, H., Green, J. S., Jass, J. R., Weber, J. L., Leach, F. S., *et al.* Genetic mapping of a locus predisposing to human colorectal cancer. Science (Wash. DC), *260:* 810–812, 1993.
51. Fishel, R., Lescoe, M. K., Rao, M. R., Copeland, N. G., Jenkins, N. A., Garber, J., Kane, M., and Kolodner, R. The human mutator gene homolog *MSH2* and its association with hereditary nonpolyposis colon cancer. Cell, *75:* 1027–1038, 1993.
52. Leach, F. S., Nicolaides, N. C., Papadopoulos, N., Liu, B., Jen, J., Parsons, R., Peltomaki, P., Sistonen, P., Aaltonen, L. A., Nystrom-Lahti, M., *et al.* Mutations of a mutS homolog in hereditary nonpolyposis colorectal cancer. Cell, *75:* 1215–1225, 1993.
53. Fujita, M., Enomoto, T., Yoshino, K., Nomura, T., Buzard, G. S., Inoue, M., and Okudaira, Y. Microsatellite instability and alterations in the *hMSH2* gene in human ovarian cancer. Int. J. Cancer, *64:* 361–366, 1995.
54. Modrich, P., and Lahue, R. Mismatch repair in replication fidelity, genetic recombination, and cancer biology. Annu. Rev. Biochem., *65:* 101–133, 1996.
55. Giannakakou, P., Poy, G., Zhan, Z., Knutsen, T., Blagosklonny, M. V., and Fojo, T. Paclitaxel selects for mutant or pseudo-null p53 in drug resistance associated with tubulin mutations in human cancer. Oncogene, *19:* 3078–3085, 2000.
56. Warnick, C. T., Dabbas, B., Ford, C. D., and Strait, K. A. Identification of a p53 response element in the promoter region of the *hMSH2* gene required for expression in A2780 ovarian cancer cells. J. Biol. Chem., *276:* 27363–27370, 2001.